Article

Study on the Shale Hydration Inhibition Performance of Triethylammonium Acetate

Yuanzhi Qu [1], Ren Wang [1,2,*], Shifeng Gao [1], Hongjun Huang [1], Zhilei Zhang [1], Han Ren [1], Yuehui Yuan [1], Qibing Wang [1,2], Xiangyun Wang [3] and Weichao Du [3,*]

[1] CNPC Engineering Technology R & D Company Limited, Beijing 102206, China; quyz_dri@cnpc.com.cn (Y.Q.); gaosfdr@cnpc.com.cn (S.G.); huanghj_dri@cnpc.com.cn (H.H.); zhangzhidr@cnpc.com.cn (Z.Z.); renhandr@cnpc.com.cn (H.R.); yuanyhdr@cnpc.com.cn (Y.Y.); wangqbdr@cnpc.com.cn (Q.W.)
[2] Department of Petroleum Engineering, China University of Petroleum (East China), Qingdao 266580, China
[3] Shaanxi Province Key Laboratory of Environmental Pollution Control and Reservoir Protection Technology of Oilfields, School of Chemistry and Chemical Engineering, Xi'an Shiyou University, Xi'an 710065, China; 18298818107@163.com
* Correspondence: wangrdr@cnpc.com.cn (R.W.); duweichao@xsyu.edu.cn (W.D.)

Abstract: Shale inhibitor is an additive for drilling fluids that can be used to inhibit shale hydration expansion and dispersion, and prevent wellbore collapse. Small molecular quaternary ammonium salt can enter the interlayer of clay crystal, and enables an excellent shale inhibition performance. In this paper, a novel ionic shale inhibitor, triethylammonium acetate (TEYA), was obtained by solvent-free synthesis by using acetic acid and triethylamine as raw materials. The final product was identified as the target product by Fourier transform infrared spectroscopy (FT-IR). The inhibition performance of TEYA was studied by the mud ball immersion test, linear expansion test, rolling recovery test and particle size distribution test. The results demonstrated that the shale inhibitor shows a good shale hydration inhibition performance. The inhibition mechanism was studied by FT-IR and X-ray diffraction (XRD), respectively; the results showed that triethylammonium acetate TEYA could enter the crystal layer of clay and inhibit it through physical adsorption.

Keywords: drilling fluids; hydration swelling; shale inhibitor; shale gas

1. Introduction

With the development of oil and gas exploration to deep wells, ultra-deep wells, offshore wells and wells in complex sections [1,2], a series of drilling problems caused by the hydration expansion and dispersion of shale, such as wellbore instability, bit mud bag and borehole purification, would occur frequently, which increases the drilling difficulty and non-operation time of the oil industry [3–6]. Drilling fluid, commonly known as the blood of drilling engineering, plays the role of suspending drilling cuttings, cleaning and cooling the bit, balancing formation pressure, reservoir protection, and maintaining wellbore stability. According to different mobile phases, drilling fluids can be divided into water-based drilling fluids, oil-based drilling fluids and synthetic-based drilling fluids. Water-based drilling fluids have the advantages of less components, a simple preparation process, environmental protection and low cost, which make them widely used all over the world. The performance of drilling fluid plays a decisive role in the stability of wellbore; therefore, special requirements are put forward for the inhibition of the drilling fluid system [7–10].

Adding shale inhibitor to drilling fluid can prevent wellbore collapse to a certain extent. There are two main action mechanisms of inhibitors [11–13]. One is that inhibitors are wrapped on the surface of shale to separate it from water. Another way is that the inhibitor enters the clay crystal layer, the water between the clay crystal layers is replaced, and the inhibitor is adsorbed inside the crystal layer, so as to play an excellent inhibition

effect [14–17]. The high molecular weight inhibitors will play the role of wrapping inhibition, which have a certain impact on the performance of drilling fluids, so its application is greatly limited. However, intercalation inhibitors gradually show a good development prospect in shale inhibitors because of their unique molecular structure advantages [18–20].

The commonly used shale inhibitors mainly include inorganic salts, asphalts, polymers and humic acids, but these shale inhibitors have some shortcomings; for example, asphalt is not conducive to environmental protection, silicate will make the rheology of the system difficult to control, glycosides cannot solve the drilling problem of active shale, etc. [21–26]. In recent years, amine-based drilling fluid has become the focus of petroleum researchers all over the world because of its environmental protection and low cost. Its essence is that amine (ammonium) shale inhibitor is added to drilling fluid. Ammonium-based shale inhibitors are usually prepared by an acid–base reaction between small molecular weight secondary tertiary amine and matrix acid. They have low molecular weight and low cost. They are used in drilling fluid and oil production, but their economy and temperature resistance still need to be further improved.

Based on the above analysis, a new ionic shale inhibitor triethylammonium acetate was developed with acetic acid and triethylamine as raw materials. Its structure was determined by infrared spectroscopy, its inhibition performance was comprehensively studied, and its inhibition mechanism was analyzed.

2. Experimental

2.1. Materials

Triethylamine, acetic acid, acetone, and absolute ethanol were purchased from Chengdu Kelong Chemical Reagent Factory (Chengdu, China) (the above reagents were analytically pure), and sodium bentonite (Na-MMT) was purchased from Xinjiang Xiazijie Bentonite Co., Ltd. (Tacheng, China).

2.2. Preparation of TEYA

Triethylamine (0.25 mol) was added into a three-neck flask, then acetic acid (0.2 mol) was slowly added with stirring, and then heated at the temperature required until the reaction was completed. After the reaction, the reaction solution was recrystallized with a mixture of ethyl acetate and anhydrous ethanol (volume ratio 8:2). TEYA was left to stand for 24 h to obtain an acicular white solid. The solid was vacuum dried at 45 °C for 8 h and TEYA was obtained. The chemical formula and the synthetic route of TEYA is shown in Scheme 1.
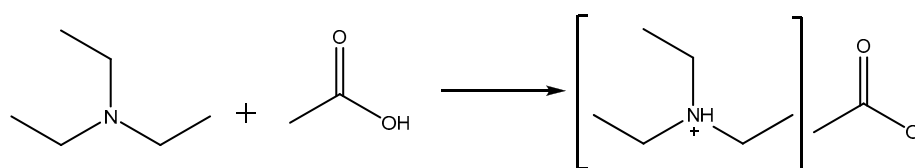
Scheme 1. The synthetic route of triethylammonium acetate (TEYA).

2.3. Inhibition Performance Study

2.3.1. Mud Ball Immersing Tests

Bentonite (50 g) was added to 25 g distilled water and stirred evenly, which was used to make a 30 g mud ball. Then, the mud ball was immersed in inhibitor solutions, and the change in the mud ball size was observed after a period of time.

2.3.2. Linear Expansion Tests

A total of 10 g Na-MMT dried at 105 °C was compressed at 10 MPa for 5 min by using a pressing machine, and the swelling height of Na-MMT was tested using a shale swelling instrument.

2.3.3. Rolling Recovery Tests

Mesh shale samples (50 g) were put into the high-temperature aging tanks filled with 350 mL solutions. The hot-rolling tests were carried out at 100 °C for 16 h. When these experiments were completed, the shale samples were carefully rinsed and filtered by a 40-mesh sieve, then dried to constant weight at 105 °C, and weighed. We calculated the hot rolling recovery rate by the equation as below:

$$R = \frac{M}{50} \times 100\%$$

where *M* is the recycling mass, g, and *R* is the rolling recovery rate, %.

2.3.4. Particle Distribution Tests

Different types of inhibitors were added to 350 mL 4% Na-MMT based slurry and fully stirred. The effect of inhibitor on the particle size of bentonite was tested after 24 h. Particle size analysis was measured with a laser diffraction technique (HORIBA, Kyoto, Japan). The operating temperature was 25 °C, the circulation speed was 2000 r/min, the ultrasonic system was 40 Hz, 70 W, and the stirring speed was 100–475 rpm.

2.4. Inhibition Mechanism Study

2.4.1. Fourier Transform Infrared Spectroscopy (FT-IR) Analysis

The Na-MMT treated with 1.2% triethylammonium acetate (TEYA) was centrifuged and filtered. During the filtration process, the Na-MMT was carefully rinsed by the mixed solution of absolute ethanol and ethyl acetate. The obtained Na-MMT was vacuum dried at 50 °C for 24 h and then stored in a closed manner. The prepared sample powder was mixed with KBr and pressed into pellets for FT-IR analysis. The FT-IR spectra in the wavelength range of 4000–500 cm^{-1} were recorded by a WQF-520 Fourier transform infrared spectrometer (Thermo Electron Co., Waltham, MA, USA).

2.4.2. X-ray Diffraction (XRD) Analysis

Na MMT (1 g) was added into 100 mL 1.2% TEYA solutions. The solutions were stirred for 2 h and then stirred at high speed for 30 min. After it was centrifuged, the bottom precipitation was washed, filtered and dried it at 50 °C for XRD tests. X-ray diffraction tests were performed on an X Pert PRO MPD diffractometer. Scans were taken from a 2θ angle from 3° to 20°, step size 0.1, and scan time per step of 10 s.

3. Results and Discussion

3.1. FT-IR Analysis

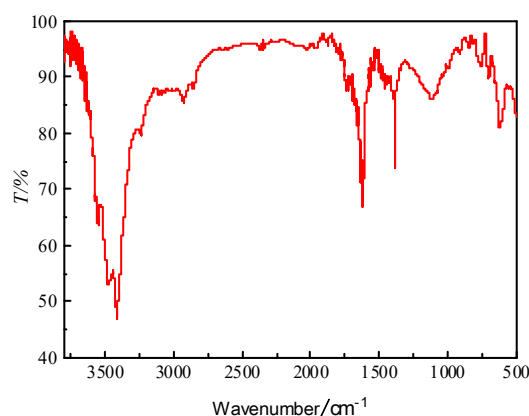The results of TEYA are shown in Figure 1.

Figure 1. The Fourier transform infrared spectroscopy (FT-IR) spectrum of TEYA.

It can be seen from Figure 1 that a strong and wide absorption peak appeared near 3485 cm^{-1}, which was the stretching vibration absorption peak of -COOH; 2850 cm^{-1} was the stretching vibration absorption peak of C-H bond in -CH$_2$- and -CH$_3$; and the peak at 1630 cm^{-1} was the stretching vibration of C-N. According to the above analysis, the synthetic product was the target product [27–30].

3.2. Mud Ball Immersing Tests

The hydration swelling tests of the inhibitor on the mud ball was studied, and the results are shown in Figure 2.
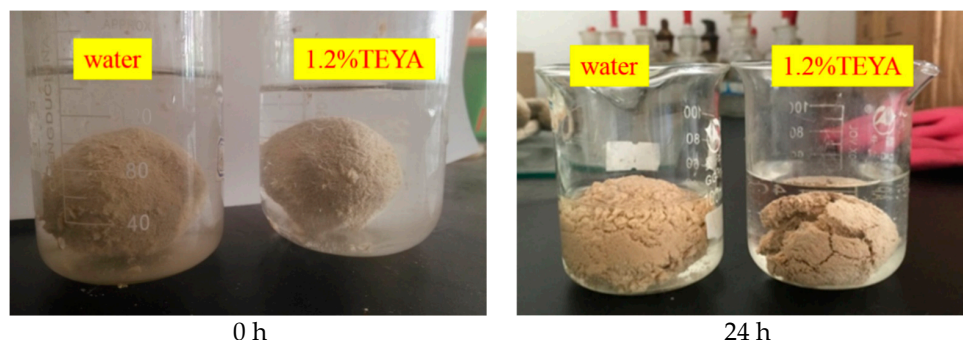

Figure 2. The status of mud balls immersed in different fluids.

It can be seen from Figure 2 that the final shape of the two mud balls was very different after immersing in different solutions for a period of time. The mud ball in water presented as expanded and broken; however, the mud ball in inhibitor solutions was relatively intact, indicating that the shale inhibitor shows an obvious inhibitory effect on the hydration of shale. This experiment directly proved that shale inhibitor TEYA could effectively prevent the hydration expansion of shale [31].

3.3. Linear Expansion Tests

The linear swelling effect of 1.2% inhibitor on shale was studied, and the experimental results are shown in Table 1.

Table 1. Linear swelling tests of shale.

Experiment Number	Test Solution	Height/mm	Swelling/mm	Swelling Rate/%
1	TEYA	11.04	2.93	26.53985507
4	KCl	10.96	3.45	31.47810219
5	Water	11.84	6.15	51.94256757

The main reason for swelling of Na-MMT is that water molecules enter into the crystal layer of minerals and the cation exchange of bentonite minerals, which increases the crystal layer spacing of bentonite. It can be seen from Table 1 that the prepared inhibitor showed the most obvious inhibitory effect on shale swelling, followed by potassium chloride (KCl). The above experimental results showed that KCl also had a certain inhibitory effect; the reason was that the diameter of K$^+$ was equivalent to the diameter of the hexagonal oxygen ring on the bottom of the clay silica tetrahedron, and the hydration energy of K$^+$ was small, which was easily inserted into the clay crystal layer. Therefore, Ca^{2+} and Na$^+$ with hydration radius and hydration energy greater than K$^+$ can be replaced. K$^+$ entering the hexagonal oxygen ring can be firmly connected with the clay wafer, and it was not easy to separate and inhibit the hydration expansion of the shale. TEYA can play an inhibition role through the synergistic effect of crystal layer substitution and concentration difference, so as to play a nice shale hydration inhibition effect [32–34].

3.4. Rolling Recovery Tests

The rolling recovery rates of shale in different solutions were compared to evaluate the inhibition performance of TEYA, as shown in Figure 3.
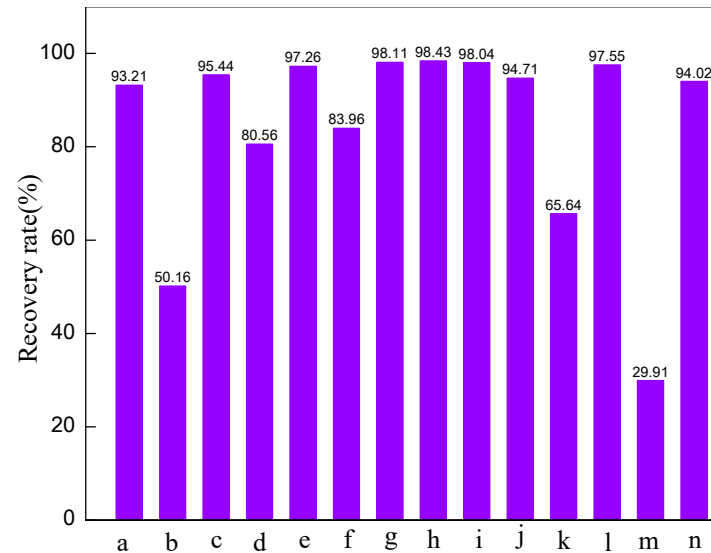

Figure 3. Effect of different inhibitors on the rolling recovery rate of shale (a, 2 %TEYA; b, water; c, 3% polydimethylamine; d, 5% emulsified asphalt; e, 5# white oil; f, 3% small cation; g, 2# oil-based drilling fluids; h, 3# oil-based drilling fluids; i, 5% KCl; j, 5%KCl+ 5% emulsified asphalt; k, 1% CaCl$_2$; l, 5% K$_2$SiO$_3$; m, 5% FeCl$_3$).

As can be seen from Figure 3, the rolling recovery of 5% FeCl$_3$ was lower than 40% and distilled water was only about 50%; the others were higher than 60%. The highest rolling recoveries were 5# white oil, oil-based drilling fluids, 5% potassium sorbate, 5% KCl + 5% emulsified asphalt, 5% K$_2$SiO$_3$, 5% KCl, 1% CaO and TEYA (93.21%). It can be seen that TEYA demonstrated a good inhibition performance.

3.5. Particle Distribution Tests

The median diameter and average diameter of the water group were compared with those with added TEYA to study the adsorption of TEYA on clay. The results are shown in Figure 4.
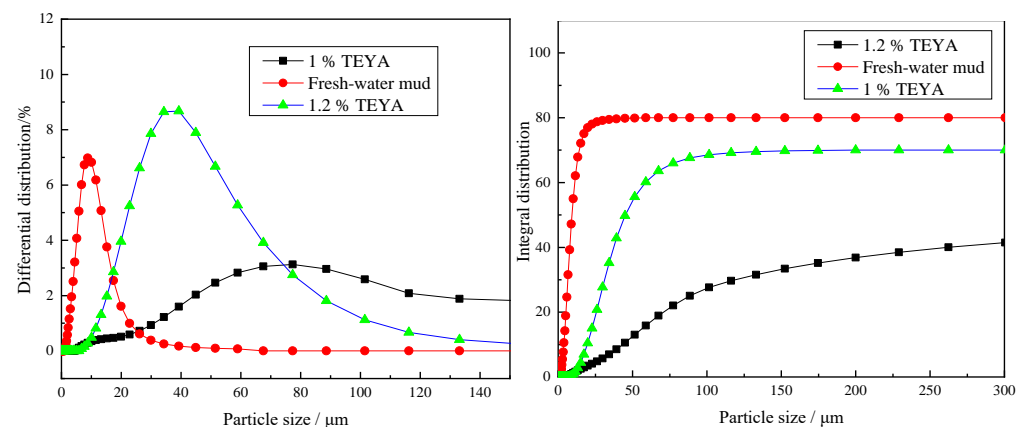

Figure 4. The differential distribution of bentonite treated by several anti-swelling agents: differential distribution/% (**left**); integral distribution (**right**).

According to Figure 4, the pitch diameter of water-based slurry was 8.05068 μm and the average diameter was 21.80842 μm. When the inhibitor was added, the median diameter was raised to 56.19773 μm and the average diameter was raised to 60.04097 μm. It can be seen that the particle diameter obviously increased, which played a certain role in inhibiting the hydration and dispersion of shale.

3.6. Inhibition Mechanism Study

The interaction between Na-MMT and clay was studied by FT-IR. Figure 5 shows the infrared spectra of Na MMT, TEYA and TEYA/Na-MMT.
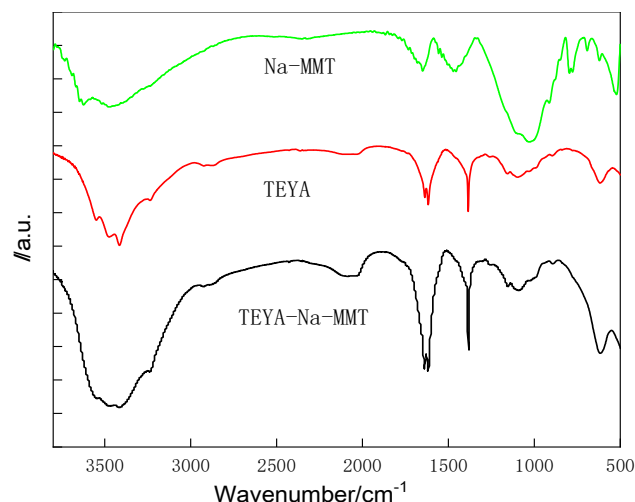

Figure 5. FT-IR spectra of Na-MMT, TEYA and Na-MMT/TEYA.

For the curve of Na-MMT, 3451 cm^{-1}, 1020 cm^{-1} and 1645 cm^{-1} correspond to the absorption peaks of -OH stretching vibration, Si-O stretching vibration and variable angle vibration of interlayer water molecules in bentonite, respectively [35]. The infrared spectra of TEYA/Na-MMT contained all the characteristic absorption peaks of the TEYA and Na-MMT, and no new peak appeared, which indicated that TEYA and Na-MMT were effectively combined together. However, the position of the absorption peak of Na-MMT was changed slightly. The variable angle vibration absorption peak of water molecules in bentonite had a red shift from 1645 cm^{-1} in low frequency to 1613 cm^{-1} in high frequency, and the peak width had narrowed and the peak strength was weakened, which indicated that the interlayer water of Na-MMT had been greatly reduced. Since TEYA contains quaternary ammonium salt, it is beneficial for TEYA to squeeze out the water molecules between the crystalline layers of bentonite, and therefore presents a nice inhibitory performance [35,36].

The XRD of dry Na-MMT treated with 1.2 wt% TEYA is shown in Figure 6. From Figure 6 we can see that the crystal layer spacing of dry Na-MMT is 1.28 nm [36], and the crystal layer spacing of TEYA/Na MMT is changed to 1.47 nm, which indicated that TEYA had successfully entered into the clay crystal layer and expanded the crystal layer spacing. Due to the occurrence of lattice substitution, the clay surface was negatively charged. The positively charged quaternary ammonium group on TEYA can ensure its strong adsorption on the clay. The molecular weight of TEYA was small and can enter the Na-MMT crystal layer to pull the crystal layer spacing.
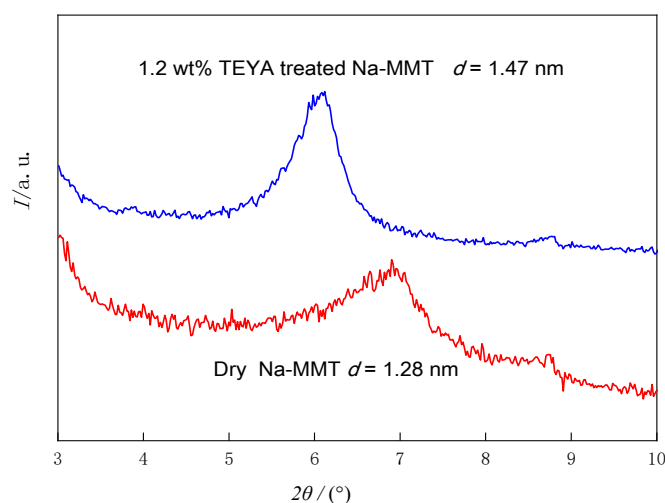
Figure 6. X-ray diffraction (XRD) of dry Na-MMT and TEYA/Na-MMT.

The inhibition mechanism is shown in Figure 7. In the water environment, water molecules increased the spacing of Na-MMT layers, and TEYA entered into the clay crystal layer to replace water molecules, so as to effectively prevent the hydration and expansion of clay [36].
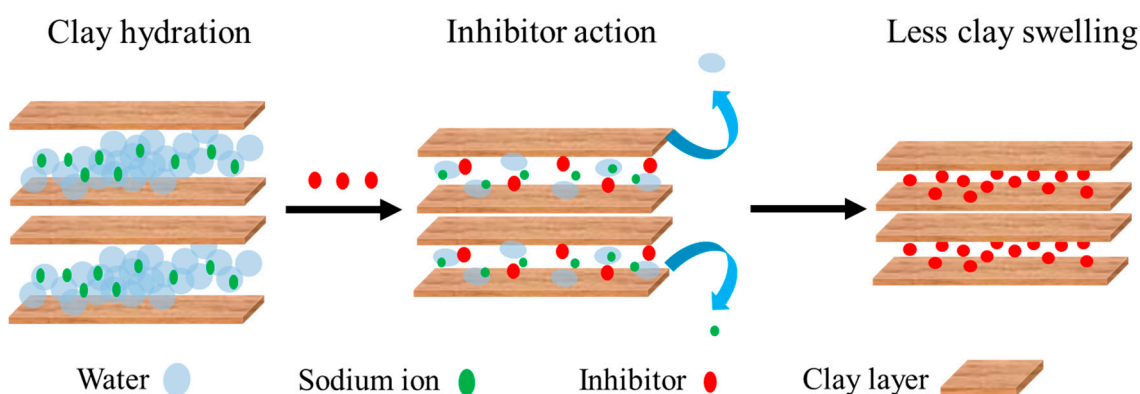

Figure 7. Inhibition mechanism of TEYA.

4. Conclusions

In this paper, a new ionic shale inhibitor TEYA was obtained by solvent-free synthesis with acetic acid and triethylamine as raw materials. The final product was identified as the target product by FT-IR. The mud ball immersion test shows that the mud ball in the inhibitor solution was relatively intact after 24 h. The linear expansion experiment showed that the linear expansion rate of clay in the inhibitor solution is only 26.54% after 16 h, the rolling recovery rate of shale in the inhibitor solution was as high as 93.21%, and the average particle size of clay in the inhibitor solution was 60.04097 μm. The results show that the shale inhibitor had a certain shale inhibition effect.

Author Contributions: Conceptualization, Y.Q.; methodology, Y.Y.; software, Y.Y.; validation, H.R.; formal analysis, R.W. and Q.W.; investigation, R.W. and S.G.; resources, X.W.; data curation, Z.Z.; writing—original draft preparation, H.H., Z.Z. and W.D.; writing—review and editing, Y.Q., Q.W., X.W. and W.D.; supervision, S.G and H.H.; project administration, Q.W. and W.D.; funding acquisition, R.W. and H.R. All authors have read and agreed to the published version of the manuscript.

Conflicts of Interest: The authors declare no conflict of interest.

References

1. Lai, N.J.; Tang, L.; Jia, N.; Qiao, D.Y.; Chen, J.L.; Wang, Y.; Zhao, X.B. Feasibility study of applying modified nano-SiO_2 hyperbranched copolymers for enhanced oil recovery in low-mid permeability reservoirs. *Polymers* **2019**, *11*, 1483. [CrossRef] [PubMed]

2. Hong, S.H.; Jo Jin, H.; Choi, M.J.; Jang, H.W.; Kim Ju, Y.; Hwang, W.R.; Kim, S.Y. Influence of MoS_2 nanosheet size on performance of drilling mud. *Polymers* **2019**, *11*, 321. [CrossRef] [PubMed]

3. Wilson, M.J.; Wilson, L. Clay mineralogy and shale instability: An alternative conceptual analysis. *Clay Miner.* **2014**, *49*, 127–145. [CrossRef]

4. Anderson, R.L.; Ratcliffe, I.; Greenwell, H.C.; Williams, P.A.; Cliffe, S.; Coveney, P.V. Clay swelling-A challenge in the oilfield. *Earth-Sci. Rev.* **2010**, *98*, 201–216. [CrossRef]

5. Gholami, R.; Elochukwu, H.; Fakhari, N.; Sarmadivaleh, M. A review on borehole instability in active shale formations: Interactions, mechanisms and inhibitors. *Earth-Sci. Rev.* **2018**, *177*, 2–13. [CrossRef]

6. Du, W.; Wang, X.; Chen, G.; Zhang, J.; Slaný, M. Synthesis, property and mechanism analysis of a novel polyhydroxy organic amine shale hydration inhibitor. *Minerals* **2020**, *10*, 128. [CrossRef]

7. Rana, A.; Arfaj, M.K.; Saleh, T.A. Advanced developments in shale inhibitors for oil production with low environmental footprints: A review. *Fuel* **2019**, *247*, 237–249. [CrossRef]

8. Ahmed, H.M.; Kamal, M.S.; Al-Harthi, M. Polymeric and low molecular weight shale inhibitors: A review. *Fuel* **2019**, *251*, 187–217. [CrossRef]

9. Gou, S.H.; Yin, T.; Liu, K.; Guo, Q.P. Water-soluble complexes of an acrylamide copolymer and ionic liquids for inhibiting shale hydration. *New J. Chem.* **2015**, *39*, 2155–2161. [CrossRef]

10. Liu, X.J.; Liu, K.; Gou, S.H.; Liang, L.X.; Luo, C.; Guo, Q.P. Water-soluble acrylamide sulfonate copolymer for inhibiting shale hydration. *Ind. Eng. Chem. Res.* **2014**, *53*, 2903–2910. [CrossRef]

11. Jia, H.; Huang, P.; Wang, Q.X.; Han, Y.G.; Wang, S.Y.; Zhang, F.; Pan, W.; Lv, K.H. Investigation of inhibition mechanism of three deep eutectic solvents as potential shale inhibitors in water-based drilling fluids. *Fuel* **2019**, *244*, 403–411. [CrossRef]

12. Zhao, X.; Qiu, Z.S.; Zhang, Y.J.; Zhong, H.Y.; Huang, W.A.; Tang, Z.C. Zwitterionic polymer P(AM-DMC-AMPS) as a low-molecular-weight encapsulator in deepwater drilling fluid. *Appl. Sci.* **2017**, *7*, 594. [CrossRef]

13. Ma, X.; Zhu, Z.; Shi, W.; Hu, Y. Synthesis and application of a novel betaine-type copolymer as fluid loss additive for water-based drilling fluid. *Colloid Polym. Sci.* **2017**, *295*, 53–66. [CrossRef]

14. Zhao, Y.-F.; Zhang, P.-B.; Sun, J.; Liu, C.-J.; Yi, Z.; Zhu, L.-P.; Xu, Y.-Y. Versatile antifouling polyethersulfone filtration membranes modified via surface grafting of zwitterionic polymers from a reactive amphiphilic copolymer additive. *J. Colloid Interface Sci.* **2015**, *448*, 380–388. [CrossRef] [PubMed]

15. Morimoto, N.; Wakamura, M.; Muramatsu, K.; Toita, S.; Nakayama, M.; Shoji, W.; Suzuki, M.; Winnik, F.M. Membrane Translocation and Organelle-Selective Delivery Steered by Polymeric Zwitterionic Nanospheres. *Biomacromolecules* **2016**, *17*, 1523–1535. [CrossRef]

16. Vu-Bac, N.; Lahmer, T.; Zhuang, X.; Nguyen-Thoi, T.; Rabczuk, T. A software framework for probabilistic sensitivity analysis for computationally expensive models. *Adv. Eng. Softw.* **2016**, *100*, 19–31. [CrossRef]

17. Vu-Bac, N.; Rafiee, R.; Zhuang, X.; Lahmer, T.; Rabczuk, T. Uncertainty quantification for multiscale modeling of polymer nanocomposites with correlated parameters. *Compos. Part B Eng.* **2015**, *68*, 446–464. [CrossRef]

18. Vu-Bac, N.; Silani, M.; Lahmer, T.; Zhuang, X.; Rabczuk, T. A unified framework for stochastic predictions of mechanical properties of polymeric nanocomposites. *Comp. Mater. Sci.* **2015**, *96*, 520–535. [CrossRef]

19. Vu-Bac, N.; Lahmer, T.; Zhang, Y.; Zhuang, X.; Rabczuk, T. Stochastic predictions of interfacial characteristic of polymeric nanocomposites (PNCs). *Compos. Part B Eng.* **2014**, *59*, 80–95. [CrossRef]

20. Pu, X.L.; Du, W.C.; Sun, J.S.; Luo, X.; Zhang, H.D. Synthesis and application of a novel polyhydroxy amine clay anti-swelling agent. *Petrochem. Technol.* **2016**, *45*, 595–600.

21. Silva, F.; Siopa, F.; Figueiredo, B.; Gonçalves, A.; Pereira, J.L.; Gonçalves, F.; Coutinho, J.; Afonso, C.; Ventura, S. Sustainable design for environment-friendly monoand dicationic cholinium-based ionic liquids. *Ecotox. Environ. Safe* **2014**, *108*, 302–310. [CrossRef] [PubMed]

22. Slaný, M.; Jankovič, Ľ.; Madejová, J. Structural characterization of organo-montmorillonites prepared from a series of primary alkylamines salts: Mid-IR and near-IR study. *Appl. Clay Sci.* **2019**, *176*, 11–20. [CrossRef]

23. Uranta, K.G.; Rezaei-Gomari, S.; Russell Paul-Hamad, F. Studying the effectiveness of polyacrylamide (PAM) application in hydrocarbon reservoirs at different operational conditions. *Energies* **2018**, *11*, 2201. [CrossRef]

24. Wang, Z.H.; Qiu, Y.L.; Guo, P.; Du, J.F.; Liu, H.; Hu, Y.S.; Zeng, F.H. Experimental Investigation of the Damage Mechanisms of Drilling Mud in Fractured Tight gas Reservoir. *J. Energy Resour. Technol.* **2019**, *141*, 092907. [CrossRef]

25. Caglar, B.; Topcu, C.; Coldur, F.; Sarp, G.; Caglar, S.; Tabak, A.; Sahin, E. Structural, thermal, morphological and surface charge properties of dodecyl trimethylammonium-smectite composites. *J. Mol. Struct.* **2016**, *1105*, 70–79. [CrossRef]

26. Madejová, J.; Komadel, P. Baseline studies of the Clay Minerals Society source clays: Infrared methods. *Clays Clay Miner.* **2001**, *49*, 410–432. [CrossRef]

27. Madejová, J.; Sekeráková, Ľ.; Bizovská, V.; Slaný, M.; Jankovič, Ľ. Near-infrared spectroscopy as an effective tool for monitoring the conformation of alkylammonium surfactants in montmorillonite interlayers. *Vib. Spectrosc.* **2016**, *84*, 44–52. [CrossRef]

28. Júnior, L.P.C.; Silva, D.B.R.; Aguiar, M.F.; Melo, C.P.; Alves, K.G.B. Preparation and characterization of polypyrrole/organophilic montmorillonite nanofibers obtained by electrospinning. *J. Mol. Liq.* **2019**, *275*, 452–462. [CrossRef]

29. Adewole, J.K.; Najimu-Musa, O. A Study on the Effects of Date Pit-Based Additive on the Performance of Water-Based Drilling Fluid. *J. Energy Resour. Technol.* **2019**, *140*, 052903. [CrossRef]

30. Zhao, X.; Qiu, Z.S.; Wang, M.L.; Huang, W.A.; Zhang, S.F. Performance Evaluation of a Highly Inhibitive Water-Based Drilling Fluid for Ultralow Temperature Wells. *J. Energy Resour. Technol.* **2017**, *140*, 012906. [CrossRef]

31. Du, W.C.; Pu, X.L.; Sun, J.S.; Luo, X.; Zhang, Y.N.; Li, L. Synthesis and evaluation of a novel monomeric amine as sodium montmorillonite swelling inhibitor. *Adsorpt. Sci. Technol.* **2018**, *36*, 655–668. [CrossRef]

32. Pérez, A.; Montes, M.; Molina, R.; Moreno, S. Modified clays as catalysts for the catalytic oxidation of ethanol. *Appl. Clay Sci.* **2014**, *95*, 18–24. [CrossRef]

33. Li, M.C.; Wu, Q.L.; Song, K.L.; French, A.D.; Mei, C.T.; Lei, T.Z. pH-responsive water-based drilling fluids containing bentonite and chitin nanocrystals. *ACS Sustain. Chem. Eng.* **2018**, *6*, 33783–33795. [CrossRef]

34. Li, M.C.; Ren, S.X.; Zhang, X.Q.; Dong, L.L.; Lei, T.Z.; Lee, S.Y.; Wu, Q.L. Surface-chemistry-tuned cellulose nanocrystals in a bentonite suspension for water-based drilling fluids. *ACS Appl. Nano Mater.* **2018**, *1*, 7039–7051. [CrossRef]

35. Suter, J.L.; Coveney, P.V.; Anderson, R.L.; Greenwell, H.C.; Cliffe, S. Rule based design of clay-swelling inhibitor. *Energy Environ. Sci.* **2011**, *4*, 4572–4586. [CrossRef]

36. Du, W.; Slaný, M.; Wang, X.; Chen, G.; Zhang, J. The inhibition property and mechanism of a novel low molecular weight zwitterionic copolymer for improving wellbore stability. *Polymers* **2020**, *12*, 708. [CrossRef]